DISCRIMINATION OF UXO-LIKE METAL TARGETS USING WIDEBAND ELECTROMAGNETIC INDUCTION

[a]Leslie Collins, [a]Ping Gao, [a]Norbert Geng, [a]Lawrence Carin, [b]Dean Keiswetter, and [b]I. J. Won

[a]Department of Electrical and Computer Engineering, Duke University
Box 90291, Durham, NC 27708-0291
Phone: (919) 660-5260, Fax: (919) 660-5293
E-mail: lcollins@ee.duke.edu

[b]Geophex, Ltd., 605 Mercury Street, Raleigh, NC 27603-2343

Abstract Category: UXO Detection

ABSTRACT

In most fielded sensors used for UXO detection and discrimination, the energy in the output of the sensor is calculated and a decision regarding the presence or absence of a target is made using this statistic. This approach leads to excessively large false alarm rates. In our previous work, we have shown that the careful application of signal detection theory to electromagnetic induction (EMI) data results in a dramatic reduction of the false alarm rate for UXO detection applications. In this work, we utilize a decision-theoretic approach to classify metal targets using wideband EMI data. One algorithm that is presented incorporates both a theoretical model of the response of a wideband, frequency-domain sensor and the uncertainties regarding the target/sensor orientation. The performance of this algorithm has been evaluated using both simulated and experimental data. Results from both simulation and measured data indicate that incorporating the uncertainty associated with the target/sensor relative position into the processor affords a significant performance gain over a processor that simply uses the predicted response at the mean expected target position. On the average, for the targets we have considered, a 60% improvement in discrimination performance is obtained [1].

The integration of a computational model into the statistical signal processing framework along with consideration of the uncertainty in the target/sensor orientation results in a computationally intensive algorithm. Because of this fact, we have also considered several alternative processors that, while sub-optimal, have significantly lowered the computational burden. In this paper, we will describe these sub-optimal processors, discuss the underlying physical nature of the EMI-based UXO detection problem that prompted the formulation, and discuss the tradeoffs between performance degradation and computational requirements.

I. INTRODUCTION

Electromagnetic induction (EMI), ground penetrating radar (GPR) sensors and various other multi-spectral and remote sensing methods have been used to locate buried landmines and unexploded ordnance (UXO). Among these, EMI is one of the most widely used sensors for these applications. EMI sensors can effectively detect metal objects. Unfortunately, there is often a significant amount of metallic debris (clutter) present in the environment. Some of buried metallic debris can produce EMI signatures that look similar to signatures obtained from UXO, which results in a large false alarm rate. The large false alarm rate is the major limiting factor to successful UXO remediations since it results in unacceptably high costs and time required to remediate a site. Consequently, EMI sensors that utilize traditional detection algorithms based solely on the metal content suffer from high false alarm rates as well.

Clearly, in UXO detection, it is necessary to achieve high probability of detection (P_d) and low probability of false alarm (P_{fa}). This requires classification or discrimination of metal targets (UXO) from metallic clutter. In order to achieve the goal of discriminating targets of interest from other pieces of metal, several modifications to traditional EMI sensors have been considered [2][3][4][5][6]. One promising approach is to operate the EMI sensor in the frequency-domain utilizing wideband excitation. The frequency dependence of the induced fields excited by buried conducting targets can then be exploited by a detector. In our previous work [1], we considered classification of various metal objects using wideband frequency-domain EMI data. The results have shown that the optimal processor affords substantial classification performance improvement for buried metal targets. Performance improves on the average by 60% over a standard approach, which usually is a matched-filter-like processor. The development of the optimal processor integrates a numerical model of wideband frequency-domain EMI responses and a Bayesian decision-theoretic approach, which incorporates the uncertainties associated with target/sensor orientations.

However, the computational burden associated with such an approach is a serious limitation, since it requires a significant amount of calculation to obtain both the theoretical model predictions as well as the integration over environmental uncertainties. Thus, this processor cannot be considered for scenarios that require real-time decision making. Therefore, alternative approaches that are sub-optimal but require significantly less computational effort are under development. We investigated an approach which first normalizes the wideband frequency-domain EMI response then applies matched filter processor **Error! Reference source not found.**. This approach is only suitable for those objects whose aspect ratio (length divided by width) is close to one. This restriction results in signatures that are "parallel" when plotted as a function of frequency as target/sensor orientation varies. We also consider a more general model, which also utilizes the physical nature of the wideband EMI response, to reduce computational complexity. Discrimination of UXO and non-UXO objects is investigated based on this new model. The performance of each of these approaches is discussed in this paper.

II. REVIEW OF PREVIOUS WORK

In our previous work [1] we have investigated discrimination of man-made metallic targets of different dimensions and metal types under conditions where the target/sensor orientation is unknown, since the exact sensor position (where measurements are obtained) relative to the underground objects is unknown in practice. An optimal classifier was developed under the framework of Bayesian decision-theoretic approach, which integrated a forward model prediction of theoretical wideband frequency-domain EMI response of each target and the uncertainties associated with target/sensor position. The optimal classifier affords performance gains of 60% on the average over the standard matched filter processor, which does not take these uncertainties into account, using both simulated and experimental data.

In order to model the wideband EMI signature of these targets, a method of moment (MoM) analysis was used to predict the theoretical response from the targets [8]. The theoretical calculations are appropriate for highly (but not perfectly) conducting and permeable targets that can be characterized by body of revolution (BOR), *i.e.* a target that is rotationally symmetric about an axis [9]. When the exact dimensions, constitutive parameters of the target, the horizontal and vertical distance from the center of the sensor to that of the target, and frequencies of interest are specified, the theoretical wideband EMI response, which is the complex induced voltage, can be calculated. To test the effectiveness of the model, model prediction was compared to data collected from a prototype wideband frequency-domain EMI sensor, the GEM-3 [10], developed by Geophex, Ltd. A brief description of the sensor can be found in Sec. III.2.

Five man-made metal targets were used for our previous analysis: an aluminum cone, an aluminum bar-bell, an aluminum disk, a thick brass disk, and a thin brass disk. Four out of these five targets were used during experimental measurements. Twenty-one frequencies, ranging from 4kHz to 24kHz in a 1kHz spacing, were used for both simulated and measured data. The output of the sensor for a particular object is not deterministic, because not only is the electronic system subject to additive noise, but also the relative position between the sensor and underground object is uncertain. Therefore, it is assumed that the sensor is subject to a small amount of additive Gaussian noise. This assumption was verified during the experimental data acquisition. Thus, the distribution of the sensor outputs at a known height and horizontal position is a Gaussian random vector with mean equal to the theoretical prediction and variance equal to that of the additive noise. Let H_i represent the hypothesis that the ith target is present, where $i=1,\ldots,K$. The received data from the ith target can be expressed as:

$$x_{ij} = A_{ij} + n_j \tag{1}$$

where j corresponds to frequency, x_{ij} is the sensor recorded data from the ith target, A_{ij} is the model prediction for the ith target at the jth frequency at a known depth and horizontal position of the target relative to the center of the sensor, and n_j is Gaussian noise with zero mean and variance of $s_{n_j}^2$. Let q_i represent the *a priori* probability that hypothesis H_i is true. We further assumed that the cost of a correct decision is zero, and the cost of any wrong decision equals one. The optimal solution for this classification problem [11] is to decide that H_i is true if

$$\frac{p(H_i|x)}{p(H_k|x)} = \frac{q_i\, p(x|H_i)}{q_k\, p(x|H_k)} > 1 \tag{2}$$

is satisfied for any $k \neq i$, where $p(x|H_i)$ is the probability density or likelihood function of data x given H_i, $p(H_i|x)$ is the *a posteriori* distribution or discriminant function [13], and x is the received data from the sensor at a known position. x is a vector containing both the magnitude and phase information of the response, which are assumed to be independent. Since no *a priori* knowledge on the probability of a certain target present is known, a uniform prior is assumed, which results in $q_i=1/K$. Therefore, when data x is received, we decide in favor of hypothesis H_i where

$$q_i\, p(x|H_i) = \max_k \{q_k\, p(x|H_k)\} \qquad k = 1,\ldots,K. \tag{3}$$

Thus, we decide in favor of a hypothesis that has the largest *a posteriori* probability evaluated at data x among the K probability density functions. After simplification, the alternative discriminant function [13] is:

$$-(x-A_i)^T\Sigma^{-1}(x-A_i) \tag{4}$$

where x is received data from the sensor, A_i is model prediction of the response of ith target and Σ is the covariance matrix of x. Given the assumptions on the noise process, Σ is a diagonal matrix with s_n^2 on the diagonal.

The discriminant function obtained in Eqn. (4) is optimal only when a target is at a known position when all the parameters are known, and when the sensor is subject to Gaussian noise. It can be implemented as a bank of "matched" filters. Here, we refer to the filters as "matched" because (1) the noise is not identically distributed, and (2) the signals are not of equal energy. These two facts result in a formulation, which is similar to, but not identical to, the traditional matched filter x^TA_i.

Since the exact position where measurements are obtained is unknown in practice, a more accurate assumption is that the height and horizontal position are uncertain. In this case, the matched filter bank is not the optimal solution, since it does not take target/sensor position uncertainties into account. Hence, in order to obtain the optimal alternative discriminant function for the received data, integration over these uncertainties must be performed, *i.e.*

$$p(x\,|\,H_i)=\iiint p(x\,|\,H_i,h,x,y)\,p(h)\,p(x,y)\,dhdxdy \tag{5}$$

where h represents the height of the sensor from the target; x, y represent the horizontal position of the center of the target relative to the sensor; and $p(h)$ and $p(x,y)$ are the *a priori* distributions of the position variables. Here, it is assumed that the height, h, and horizontal position x, and y are independent. Monte Carlo integration was used to calculate this integral.

The performance of both the matched filter bank and the optimal classifiers was investigated using both simulated and measured data, respectively. Four cases were considered in simulations. They are (1) the target is at a known, fixed position, (2) the height of the sensor from the target is Gaussian distributed with mean of 20 cm and variance of 1.53^2 cm^2 and the sensor is right above the center of the target, (3) the horizontal position of the target relative to the center of the sensor is uniformly distributed in a 20 cm by 20 cm square and the height of the sensor is fixed, and (4) both the height and horizontal position are uncertain, following the same distributions as above. The priors placed on the uncertain positional parameters are consistent with those observed in demining applications [14].

The measured data was collected at Geophex Ltd. using the GEM-3. For each target, measurements were taken at 164 positions. The choices of these locations follow a Gaussian distribution for height and a uniform distribution for horizontal position as in the simulations. At each location, two measurements were taken so that errors in data transmission could be corrected.

Using both simulated and measured data, the optimal processor consistently affords a dramatic performance gain over the standard matched filter processor. However, because of the computational burden of the optimal processor an alternative sub-optimal approach was investigated **Error! Reference source not found.**. This processor avoids the evaluation of multi-variable integration in Eqn (5) by introducing a simple normalization operation before performing the matched filter.

For the particular class of targets (the target aspect ratio is close to one), normalizing the wideband EMI responses, which exploits the physical nature of the signals, mitigates the uncertainties of the response due to the unknown target position. In the theoretical model predictions of the wideband EMI responses for the same target at different heights and horizontal positions, a somewhat 'parallel' structure as a function of frequency is observed, as illustrated in Figure 1. The overall level varies substantially as the target/sensor orientation changes, but the basic structure of the response as a function of frequency changes only slightly. Based on this phenomenon, we hypothesized that if the wideband EMI signatures were normalized, performance could be evaluated using a processor that avoids calculating the integration over position uncertainty (as in Eqn. (5)). Then, the processor can be implemented as previously described for the matched filter case after normalization. Therefore, the outputs of the sensor were normalized to force the energy over the frequency range considered to be equal to unity. This normalization does not change the phase of the response, but the magnitude of the response after normalization is almost identical as the target/sensor orientation changes. This operation essentially decreases the uncertainties of the data collected in an uncertain environment. The sub-optimal processor takes the form of Eqn. (4), which uses the mean signature after normalization over all uncertainties as A_i for the ith target.

The results of this approach indicated that (1) for the fixed position case, performing the normalization degrades the performance of the processor, and (2) when the target positions are uncertain, better performance can be achieved if the output is normalized. In fact, the matched filter performance is quite close to the optimal classifier performance for the normalized data. This indicated that applying the sub-optimal processor to normalized data only slightly sacrifices

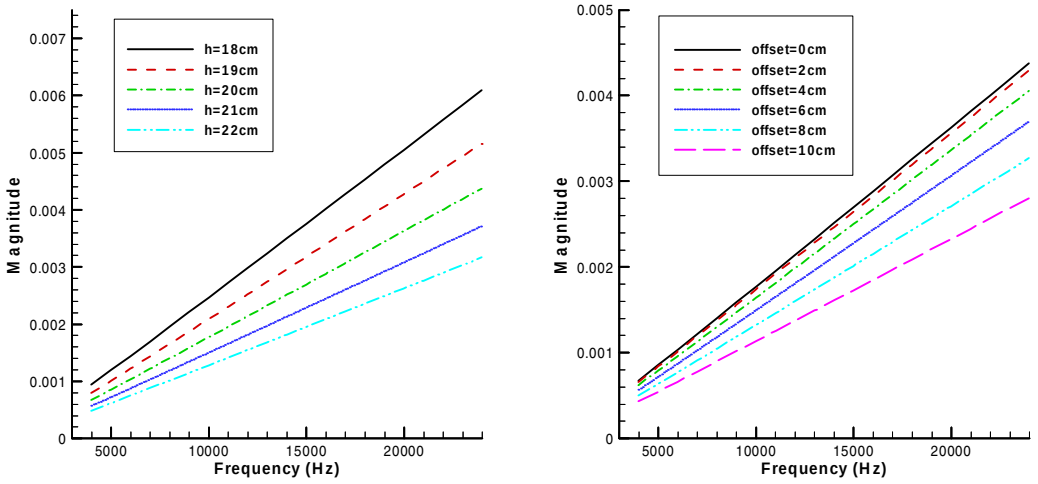

Figure 1. The wideband EMI signature of the thick brass disk while the height of the sensor (left) and the distance from the sensor to the target in a horizontal plane (right) change.

performance, but computational time is reduced significantly. It is noted that the optimal classifier operating on the normalized data outperforms the optimal classifier operating on the unnormalized data, because the normalization uncorrelates the signals to a small extent, which improves classification performance [17]. For instance, the average correlation coefficient decrease before and after normalization between the target 3 and 5 is 0.711×10^{-4}.

Experimental data also validated simulation results. The sub-optimal processor using normalized data performs better in general than the processor using raw sensor output and the optimal processor after normalization achieves better performance than the processor without normalization. This performance improvement validates the hypothesis that by normalizing the sensor data, the uncertainties associated with the sensor/target position can be decreased. Also, the performance of the sub-optimal processor operating on normalized data is very close to that of the optimal processor operating on normalized data. However, the computational load is reduced significantly by using the matched-filter-like processor. Results for the simulations and experiments described above are summarized in Tables 1 and 2.

			Probability of Correct Classification				
			Target 1	Target 2	Target 3	Target 4	Target 5
Fixed Position	No Norm.	MF/Opt.	1	1	1	1	1
	Norm.	MF/Opt.	1	.976	1	.976	1
Height Uncertain	No Norm.	MF	.832	.351	.518	.081	.620
		Opt.	.999	.857	.997	.830	1
	Norm.	MF	1	.973	1	.972	1
		Opt.	1	.977	1	.978	1
Horizontal Position Uncertain	No Norm.	MF	.804	.411	.573	.085	.655
		Opt.	1	.828	1	.810	.999
	Norm.	MF	1	.849	1	.754	1
		Opt.	1	.866	1	.810	1
Both Height & Horiz. Position Uncertain	No Norm.	MF	.758	.340	.506	.073	.492
		Opt.	.994	.701	.990	.700	.996
	Norm.	MF	1	.848	1	.759	1
		Opt.	1	.879	1	.823	1

Table 1. The performance of the various processor before and after normalization using simulated data when (1) the target position is known and fixed, (2) the height of the sensor is Gaussian distributed with mean of 20 cm and variance of 1.532 cm2, the horizontal position is fixed, (3) the horizontal position is uniformly distributed in a 20 cm by 20 cm square and height is fixed, and (4) both height and horizontal position are random, following the distributions mentioned above. In the table, 'No Norm.' means processing occurred without normalization, 'Norm.' means processing followed normalization. 'Opt.' means optimal classifier, and 'MF' indicates matched filter-like processor.

	Target 2	Target 3	Target 4	Target 5
Opt. Proc., No Norm.	0.91	0.77	0.69	0.81
Opt. Proc., Norm.	0	0.98	1	0.99
MF, No Norm.	0.23	0.24	0.03	0.14
MF, Norm.	1	0.99	0.89	0.83

Table 2. The performance of the sub-optimal and optimal processors before and after normalization evaluated on measured data. In the table, 'MF' represents the matched filter, or sub-optimal processor, 'No Norm.' means processing occurred without normalization, 'Opt. Proc.' represents the optimal processor, and 'Norm.' means processing followed normalization.

Using the sub-optimal processor, computational savings are proportional to that required to evaluate the integral shown in Eqn. (5). If the computational time of the sub-optimal processor is Δ, and the integral described by Eqn. (5) is evaluated by the Monte Carlo method, and 1000 sets of random numbers representing positions are used for iterations, the optimal processor takes 1000Δ to obtain the result. The only additional computation required by the sub-optimal processor is the normalization of the data, which is a simple operation.

In summary, the model-based Bayesian decision-theoretic approach can improve performance significantly over the standard matched filter processor under the condition that the target/sensor position is uncertain. This approach requires a library of signatures for each target at all possible target positions and evaluation of a multi-variable integral. Such an approach is computationally expensive. Performing normalization can help reduce computational complexity for targets whose signatures exhibit a parallel structure while target/sensor position changes, however this is a fairly restrictive assumption given the general class of UXO targets.

III. RESONANCE-BASED APPROACH

1. Background

Since for general targets the frequency-domain EMI response does not simply scale when the target/sensor orientation changes, the parallel structure of the response (shown in Figure 1) while target/sensor orientation varies will no longer be observed. Thus, a simple normalization followed by a matched filter processor will not provide good performance for a more general class of targets.

Because the concept of high-Q dielectric resonances can be extended to EMI resonances of highly conducting and permeable targets (at kilohertz frequencies), the real resonant frequency for a dielectric-resonator is analogous to purely imaginary resonant frequencies for EMI resonances. The resonant frequencies correspond to first-order poles in the complex frequency plane, thus, the target transfer function can be expressed as [15]

$$H(f) = d + \sum_n \frac{a_n f}{f - j \cdot f_n} \tag{6}$$

where f represents frequency, d is a DC present when a target is ferrous, f_n is the n-th resonant frequency, a_n is the coefficient of the n-th term. This equation is valid at EMI frequencies, characterized by an operating wavelength that is very large relative to representative target dimensions. Note that f in the numerator of Eqn. (6) is motivated by a high frequency EMI limit. The resonant frequencies are functions of the dimensions, constitutive parameters of the target, *etc*. The resonant frequencies are independent of the target/sensor orientation; however, the coefficients are a function of the target/sensor orientation, *i.e.* the vertical and horizontal relative position of the target relative to the sensor. Therefore, the resonant frequencies can be used to distinguish objects. In our previous work, the targets considered were non-ferrous, the aspect ratio was close to one, and the first pole was dominant, so the response could be expressed as

$$H(f) \approx \frac{a_1 f}{f - j \cdot f_1}. \tag{7}$$

Thus, while target/sensor orientation varies, the coefficient a_1 changes, this causes the response to change in overall level, but the basic structure does not change. Therefore, when the aspect ratio is close to unity, normalization can help reduce computational complexity by mitigating the correlation across the various target signals.

In general, Eqn. (6) can represent the frequency EMI response of a highly conducting and permeable object. This can also be expressed in time-domain by performing an inverse Fourier Transform,

$$h(t) = (d + \sum_n a_n)d(t) - 2p\sum_n a_n f_n e^{-2pf_n t}u(t) \qquad (8)$$

where $d(t)$ represents the delta function, and $u(t)$ is the step function. Eqn. (8) is an approximation of the impulse response, since it is integrated over the whole frequency range, not just those valid for EMI frequencies. This more general model can be used to effect discrimination of more general targets.

2. Data description (JPG IV)

Phase IV of the UXO Detection, Identification, and Remediation Advanced Technology Demonstration (ATD) was held at Jefferson Proving Ground (JPG) in Madison, Indiana from February through October 1998 [17]. The series of JPG experiments comprises a congressionally mandated program that seeks safer, more economical, and more effective methods for finding and removing UXO. Two controlled technology demonstration areas were created by the Naval Explosive Ordnance Disposal Technology Division (NAVEODTECHDIV). Inert UXO and clutter items were emplaced at these two areas for demonstrators to test their discrimination capability. The two areas consisted of a 32-hectare area, which used by demonstrators to self test their technologies, and a 16-hectare area, which used for subsequent technology demonstrations. Ground truth of the 32-hectare self-test area was provided to demonstrators, while only target location (easting and northing) information was provided for the 16-hectare demonstration area. Several demonstrators surveyed the sites with their equipment. Geophex Ltd. is one of the demonstrators.

The UXOs emplaced include 20-mm projectiles, 57-mm projectiles, 60-mm mortars, 76-mm projectiles, 81-mm mortars, 90-mm projectiles, 105-mm projectiles, 4.2-inch mortars, 152-mm projectiles, and 155-mm projectiles. The objects were primarily comprised of steel, however, the 81-mm mortars and the 105-mm projectiles were known to also contain aluminum.

Non-UXO objects consisted of scrap metal cut to weights similar to the above ordnance types. Weights of objects ranged from less than that of a 20-mm round, 0.15 pounds, to greater than a 155-mm projectile, 142.5 pounds. They were comprised of iron and steel. Some of the non-UXO objects had aspect ratios similar to that of the UXO targets.

The data analyzed in this paper were measured using the GEM-3 sensor at JPG, which is a prototype wideband frequency-domain EMI sensor, developed by Geophex, Ltd. [10]. The sensor consists of a pair of concentric circular transmitting coils, which creates a magnetic cavity at the center, and a small circular receiving coil placed within the magnetic cavity to sense the weak secondary induced field. The transmitting coils send out a complex waveform consisting of a set of user-defined frequencies. The sensor records the in-phase and quadrature component of the complex induced magnetic field at the receiving coil.

During the experiments, eight frequencies were used: 30, 90, 210, 510, 1350, 3570, 9210, and 23,970 Hz. First, a library of GEM-3 signatures was measured consisting of all the UXO and non-UXO objects present in the 32-hectare site. For each object, data from three orientations were measured in free space. Then, the sensor was used to survey all the buried UXO and non-UXO objects in the 16-hectare area.

3. Pole estimation

As mentioned above, the resonant frequencies (poles) are characteristics that can be used to discriminate between objects. Here, we discuss the approach used to estimate the poles of the frequency-domain response using multiple target/sensor orientation data. In the GEM-3 library data, targets data from three target/sensor orientations are available for all targets. The three different orientations are the nose of UXO target 45^o up, 45^o down, and flat.

Theoretically, an infinite number of modes exists. However, in practice, one or two poles dominate the response. An iterative least-squares method was utilized to estimate the poles for each target. One set of poles was selected which bet fit the data from all three orientations. The DC shift term and coefficients (d and a_n in Eqn. (6)) remained free. In Figure 2, a comparison of the original data to the fitted data using the pole estimated is shown. Clearly, a two-pole fit is much closer to the original data than a one-pole fit. Since two poles can represent the response very well, a library of the estimated values of the two poles characterizing each UXO and non-UXO object was built.

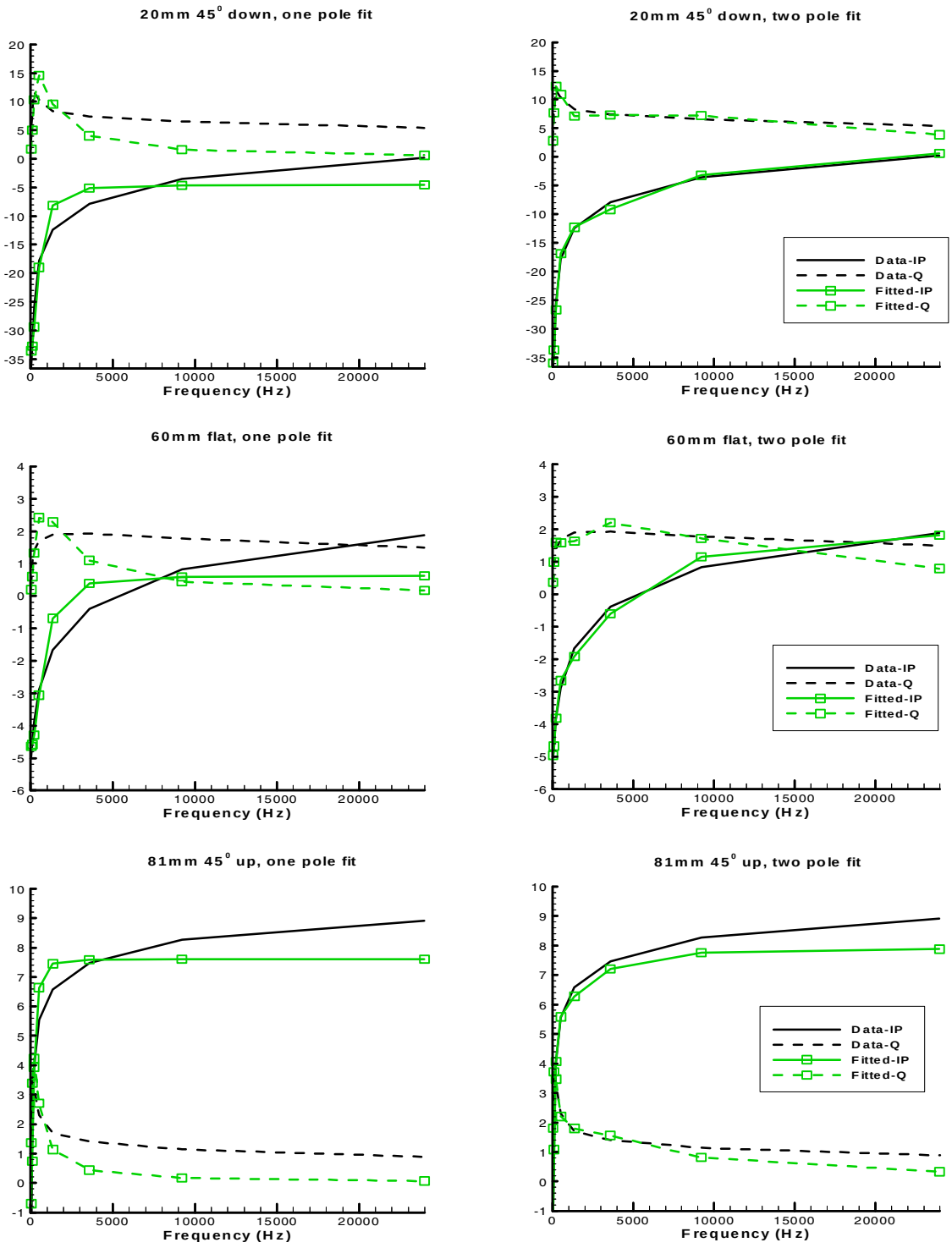

Figure 2. A comparison of fitted data using one (left) and two (right) poles to the original data for three different UXO targets and at different target orientations.

4. Detector description

After building the library of poles, each set of poles corresponding to a target is used to fit blind data. A detector, which utilizes the L2 norm of the error between fitted and original data, was implemented. The error is

$$e_j^{\,2} = \sum_{i=1}^{8} (O_i - F_i^{(j)})^2$$

where i represents the ith frequency, $i=1,\ldots,8$, O_i is the measured data from the GEM-3 at ith frequency, , $F_i^{(j)}$ is the fitted data at the ith frequency using poles for jth target, e_j^2 is the error between the original data O and the fitted data using poles of jth target. Ideally, the error corresponding to the correct target, from which the data was measured, is the minimum among all the targets. Thus, the minimum error of a blind data is considered as the detector output for this data set. The reciprocal of this value (used to avoid changing the decision rule) is used to compare to a threshold to make a decision, specifically whether the data is from a UXO target (H_1), or a non-UXO object (H_0).

5. Detector performance

Figure 3 illustrates the performance of the approach described above. The improvement in detection probability between the detector mentioned above and baseline performance of the GEM-3 sensor for this data set is over 12% at false alarm rate of 20%. The false alarm rate is decreased by 10% when detection probability is held fixed at 68% using this detector.

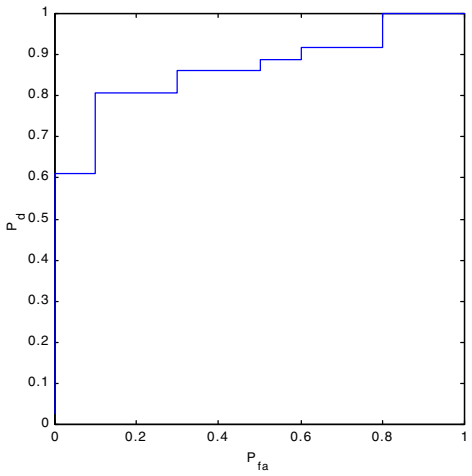

Figure 3. ROC curve of the detector discussed in Sec. III.4.

IV. DISCUSSION AND FUTURE WORK

A general model of the frequency-domain EMI response is used in this paper. By incorporating this model, the target response can be characterized by first-order poles, furthermore, a detector that utilizes the minimum error between original data and fitted data using poles corresponding to each target as decision statistic is developed and the performance of such detector is better than that of standard approach. Such a detector avoids building a library of predicted theoretical response of each target at every possible position and evaluation of multi-variable integral, thus computational complexity is reduced significantly. In the future, we will investigate other detection schemes that incorporate this model and statistics of poles of UXO and non-UXO objects.

V. ACKNOWLEDGEMENT

The work is sponsored by the Army Research Office under grant DAAH04-96-1-448 (Demining MURI) and by SERDP.

VI. REFERENCE

[1] P. Gao, L. Collins, P. Garber, N. Geng, and L. Carin, "Classification of Landmine-Like Metal Targets Using Wideband Electromagnetic Induction". Submitted to *IEEE Trans. Geoscience and Remote Sensing*, Nov. 1998.

[2] N. Geng, *et al*., Wideband Electromagnetic Induction for Metal-Target Identification: Theory, Measurement and Signal Processing. Technical Report, Duke University, Sep. 1997.

[3] L. Collins, P. Gao, and L. Carin, "An Improved Bayesian Decision Theoretic Approach for Land Mine Detection". *IEEE Trans. Geoscience and Remote Sensing*, Vol. 37, No. 2, Mar. 1998.

[4] C. E. Baum, Low Frequency Near-Field Magnetic Scattering from Highly, but Not Perfectly Conducting Bodies. Phillips Laboratory Interaction Note 499, Nov. 1993.
[5] G. D. Sower and S. P. Cave, "Detection and Identification of Mines from Natural Magnetic and Electromagnetic Resonances". *Proceedings of SPIE*. 1995. Orlando, FL.
[6] S. Vitebskiy and L. Carin, "Late-Time Resonant Frequencies of Buried Bodies of Revolution". *IEEE Trans. Antennas Propagation*, 1996. 44: p. 1575-1583.
[7] P. Gao and L. Collins, "A Comparison of Optimal and Sub-Optimal Processors for Classification of Buried Metal Objects". *IEEE Signal Processing Letters*, February 1999.
[8] R. F. Harrington, Field Computation by Moment Methods. The Macmillan Company, New York, 1968.
[9] J. R. Mautz, R. F. Harrington, "Radiation and Scattering from Bodies of Revolution". Applied Scientific Research, vol. 20, p. 405-435, June 1969.
[10] I. J. Won, D. A. Keiswetter, and D. R. Hansen, "GEM-3: A Monostatic Broadband Electromagnetic Induction Sensor". Journal of Environmental and Engineering Geophysics, 2: 53-64, Aug. 1997.
[11] J.C. Hancock and P.A. Wintz, *Signal Detection Theory*. New York: McGraw Hill, 1966. p. 80-84.
[12] H. L. Van Trees, *Detection, Estimation, and Modulation Theory*. New York: John Wiley and Sons, 1968.
[13] R. J. Schalkoff, *Pattern Recognition: Statistical, Structural and Neural Approaches*. New York: John Wiley and Sons, 1992. p. 34-43.
[14] Army FM 20-32, "Mine Countermine Operations", May 1998.
[15] L. Carin, *Wideband Time- and Frequency-Domain EMI: Phenomenology and Signal Processing*, Technical Report on U.S. Air Force Philip's Laboratory Project, Oct. 1998.
[16] J. G. Rasimas, *Signal Detection and Classification of Targets Using Multiple Aspect Angles*, Master's Thesis, Duke University, 1998.
[17] Waterways Experiment Station Report, Controlled Site Phase IV Jefferson Proving Ground Demonstration Work Plan.